

Application of 3DG/CB/MnO₂ Electrode Material in Supercapacitors

Yu Cui¹, Shengming Xu², Junwei An^{2,*}, Shaohui Yan^{3,*}

¹ School of Civil Engineering, Chongqing University, Chongqing, 400044, China

² Institute of Nuclear and New Energy Technology, Tsinghua University, Beijing, 100084, China

³ College of Environmental Science and Engineering, Taiyuan University of Technology, Taiyuan, 030024, China

*E-mail: shyan@buaa.edu.cn

Received: 26 April 2016 / Accepted: 20 May 2016 / Published: 4 June 2016

Using a three-dimensional graphene (3DG) prepared by a sol-gel method as skeleton material, and adding commercial carbon black as conductive additive, a novel composite electrode material (3DG/CB/MnO₂) is synthesized by hydrothermal method. The 3DG and 3DG/CB/MnO₂ composite are characterized by SEM and XRD. The SEM results indicate that the thickness of graphene sheets is homogeneous, and the MnO₂ nanoparticles are successfully deposited on the surface of the 3DG and carbon black to form a honeycomb structure, in which numerous pores are constructed by the graphene sheets and carbon nanotubes (CNTs). The XRD result shows that the state of the MnO₂ in the 3DG/CB/MnO₂ composite is δ -MnO₂. The electrochemical test results display that the specific capacitances are 590, 433 and 247 F/g respectively at the current densities of 0.3, 1 and 3 A/g. Whereas, the specific capacitances of the MnO₂ nanoparticles at 0.3 A/g is only 433 F/g. After the 3DG/CB/MnO₂ composite is charge-discharge for 5000 cycles at the big current densities of 30 A/g, its specific capacitance decreases to 38 F/g from 55 F/g. The capacitance retention of the 3DG/CB/MnO₂ composite reaches to 70%, implying this composite is a supercapacitor electrode material which has the prospect of industrialization.

Keywords: Three-dimensional Graphene; MnO₂; Supercapacitor; Electrode Materials

1. INTRODUCTION

The exploration of the electrode materials with high energy density, high power density and good cycle stability used in supercapacitors is of great importance for the wide commercial applications of supercapacitors. Therefore, the continuous interest in this field has shaped numerous studies. Recently, the investigation of the composite electrode materials, synthesized by the method that pseudocapacitor material or conductive polymer is loaded on the graphite is used as the skeleton

material, has been a focus of intensive research, because these composites have both the electric double layer capacitor and the Faraday pseudocapacitor [1-15]. In these materials, the good performance of the graphene in terms of conductivity, specific surface area and chemical stability is fully utilized, to promote the rapid transfer of the Faraday capacitance charge in the pseudo capacitive material or conductive polymer, which improves the energy density, power density and cycle stability of the composite electrode materials [1-8]. Moreover, the mechanical properties of the composite are enhanced by the self supported flexible carbon based material, further increasing the cycle stability [9-15].

As an atomic crystal with two-dimensional (2D) structure, the thin layer structure of the graphene is easy to reunite and stack, which greatly reduces the effective surface area of the graphene, so that the excellent characteristics of the graphene is difficult to play out. Therefore, considerable efforts have been made on the preparation of the graphene with three-dimensional (3D) structure [16-19]. The graphene with 3D structure (3DG) maintains the physicochemical properties of the graphene with 2D structure, such as large specific surface area, low weight density, high mechanical strength, excellent electronic conductivity etc. Moreover, the 3D porous with micro/nanostructures composed by the surface defects of the graphene enlarge the graphene layer spacing, which makes mass transfer fast, improving the kinetic properties of electrochemical reaction. It has been found that the composite synthesized by the 3DG and pseudocapacitive material (or conducting polymer) which employed as the electrode material for supercapacitor demonstrates a superior electrochemical performance in [20-25].

MnO₂ is considered as a promising material for the application of industrial applications, due to its wide distribution in nature, low prices and high theoretical specific capacitance (1400F/g). However, the poor conductivity of the MnO₂ pseudocapacitive materials makes the faraday charge can't be quickly charge-discharge to form an effective capacitance, resulting in the actual specific capacitance of the MnO₂ is only 236 F/g [26]. Therefore, in this work, the 3DG prepared by a sol-gel method and carbon black with low prices are employed as the skeleton material and conductive additive, MnO₂ nanoparticles are synthesized by a hydrothermal method on the surface of the graphene and carbon black. In the electrode material composed by the 3DG, carbon black and MnO₂ (3DG/CB/MnO₂), the synergistic reaction between the 3DG and MnO₂ is fully played out, which is propitious to the increase in the electrochemical performance of the 3DG/CB/MnO₂ composite. The morphology, structure and electrochemical performance of the 3DG and 3DG/CB/MnO₂ composite are characterized by SEM, XRD and the electrochemical testing methods.

2. EXPERIMENTAL

2.1 Synthesis of the 3DG

The graphene oxide is prepared by a modified Hummers method [27]. Typical procedures are as follows: firstly, 50 g expandable graphite, 25 g sodium nitrate, 500 ml sulfuric acid are added in a 2 l beaker. Then, the beaker is put in a water bath, in which the temperature is fixed at 0 °C, to prevent

the reaction temperature from reaching 10 °C. In 1 h, 300 g potassium permanganate is added into the mixture in 6 times under gently stirring. After that, the temperature of the mixture is increased to 35 °C. After holding 30 min, 920 ml distilled water is slowly dropped in the beaker. After further stirring for 1 h, the solution is set quietly for 12 h. After the mixture is maintained at 98 °C for 1 h, it is filtrated. A graphene oxide can be obtained, after the filter residue is dried.

The 3DG is prepared by a sol-gel method. Typical procedures are as follows: firstly, 50 mg graphene oxide synthesized above is dispersed in 90 ml distilled water by ultrasonic agitation for 30 min. Then, the pH of the suspension is adjusted to 9 using saturated sodium carbonate solution. Thereafter, 500 mg carbon nanotubes (CNTs) is scattered in the mixture by ultrasonic agitation for 30 min. Then, the mixed solution is moved into a 120 ml reaction kettle. After that, the reaction kettle is heated using an oven at 180 °C for 5 h. Then, the mixture is frozen at -80 °C for over 2 h. Finally, the 3DG is obtained after the frozen material is dried in the condition of low temperature and high vacuum (less than 30 Pa).

2.2 Synthesis of the 3DG/CB/MnO₂ composite

The procedures for the synthesis of the 3DG/CB/MnO₂ composite are as follows: to begin with, 1.26 g KMnO₄, 50 mg 3DG and 50 mg carbon black are scattered in 80 ml distilled water successively by magnetic stirring for 5 minutes, ultrasonic agitation for 5 min and high speed stirring for 5 min under 150,000 rpm. After that, the mixture is transferred to a hydrothermal synthesis reactor, which is then heated using an oven at 160 °C for 5 h. After the reaction is completed, the mixture is cooled down and filtrated. Finally, the 3DG/CB/MnO₂ composite is obtained, after the filter residue is dried in a vacuum drying oven at 80 °C for 12 h.

2.3 Characterization of electrode materials

The morphologies of the 3DG and 3DG/CB/MnO₂ composite are investigated by a HITACHI S-4800 scanning electron microscope (SEM). X-ray powder diffraction data of the 3DG, MnO₂ and 3DG/CB/MnO₂ composite are collected using a Rigaku Dmax 2400 X-ray diffractometer.

2.4 Electrochemical test

The electrochemical tests of the 3DG, MnO₂ and 3DG/CB/MnO₂ composite for supercapacitor are carried out at the ambient temperature using a CHI 760E electrochemical workstation (Shanghai, China). The test electrolyte is 2 M Na₂SO₄ solution, whose pH is adjusted to 9~10 by KOH solution. Fabrication of the working electrode refers to literature [28-30]. Briefly, 20 μl composite ink, prepared by mixing 20 mg tested electrode material, 5 mg carbon black, 4 ml ethanol, 30 μl PTFE emulsion and 30 μl Nafion solution (5 wt%, DuPont Corp., USA), is placed on a polished glassy carbon working electrode (Φ = 5 mm) using a microsyringe. An Ag|AgCl electrode and a sheet of platinum (2 cm²) are respectively employed as the reference electrode and counter electrode.

3. RESULTS AND DISCUSSION

3.1 Electrode materials characterization

Figure 1 shows the SEM images of the 3DG and 3DG/CB/MnO₂ composite. As can be seen from Figure 1a, 3DG contains numerous reticular porous structures constructed by the CNTs and graphene sheets, resulting in that the graphene sheets rarely agglomerate together. Moreover, there are a large number of folds and wrinkles in the graphene sheet, since the overlap between graphene layers reduce the surface energy [31,32]. Such a 3D network structure can not only effectively prevent the accumulation of the graphene sheet layer, but also is conducive to the uniform load of the MnO₂ on the surface of 3DG. Therefore, the sufficient contact between the MnO₂ nanoparticles and the electrolyte solution is ensured, which has a great effect on the increase in the electric capacity and the cycle stability of the composite material.

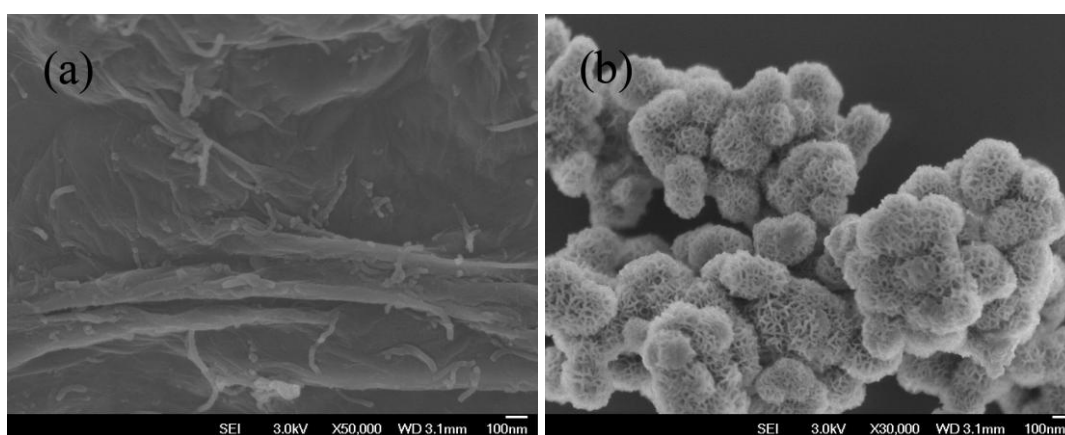


Figure 1. SEM images of the 3DG (a) and 3DG/CB/MnO₂ composite (b).

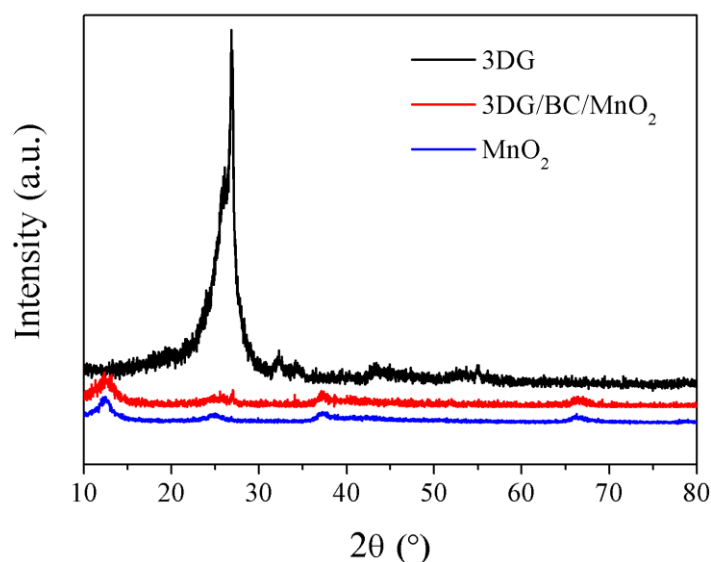


Figure 2. XRD patterns of the 3DG, MnO₂, and 3DG/CB/MnO₂ composite.

Figure 1b indicates that the surface of the 3DG/CB/MnO₂ composite exhibits perfect honeycomb, which implies that the interior of the 3DG/CB/MnO₂ composite is filled with the carbon network structure constructed by 3DG and carbon black. There is no doubt that the carbon network structure constructed by 3DG and carbon black can effectively accelerate the transfer of Faraday charge.

Figure 2 displays the XRD patterns of the 3DG, MnO₂, and 3DG/CB/MnO₂ composite. The XRD pattern of the 3DG in Figure 2 indicates that a strong diffraction peak appear at $2\theta=26.8^\circ$, which suggests that the 3DG has a high degree of crystallinity. The diffraction peak corresponds to the [002] diffraction peak of graphite, implies that the graphene sheets are of uniform thickness and good dispersion. Moreover, a series of diffraction peaks locates at $2\theta = 12, 25.7, 36.8$ and 66° , which are associated to the birnessite-type MnO₂ (δ -MnO₂) [JCPDS No. 18-0802]. However, its crystallinity is low, which may be related to the lamellar thickness of the nano MnO₂ sheet in the 3DG/CB/MnO₂ composite, causing by the preparation process of the 3DG/CB/MnO₂ composite.

3.2 Electrochemical study

The CVs of the 3DG/CB/MnO₂ composite at different scanning rate are shown in Figure 3a, which indicates that the CV curve of the 3DG/CB/MnO₂ composite at 2 mv/s scan rate presents a quasi-rectangular shape, which shows that the 3DG/CB/MnO₂ composite has the characteristics of double layer capacitance at low scan rate. As the scan rate increases from 2 to 50 mv/s, the rectangular structure of the CV curves is expanding, and the shape of the rectangle is also changed, due to the effect of the internal resistance of the electrode material on CV curve. Moreover, the capacitance performance of the 3DG/CB/MnO₂ composite decreases with the enhancement in the scanning rate [33]. Figure 3b displays the CVs of the 3DG, MnO₂ and 3DG/CB/MnO₂ composite at 200 mv/s. It can be seen from Figure 3b that the rectangular area of the 3DG/CB/MnO₂ composite is far greater compared with the 3DG and MnO₂, which indicates that the specific capacitance of the 3DG/CB/MnO₂ composite is greatly improved when the MnO₂ combined with the 3DG and carbon black. Furthermore, the rectangular area of the 3DG/CB/MnO₂ composite is greater than the sum of the rectangular areas of the 3DG and MnO₂. This result implies that the 3DG and carbon black with high conductivity can greatly promote the specific capacitance of the MnO₂. The possible reason is the carbon network structure constructed by 3DG and carbon black effectively prevents the 2D graphene sheet agglomerating to weaken the surface area of the 2D graphene, and the large specific surface and high conductivity of 3DG and carbon black makes the pseudocapacitive performance of the MnO₂ fully play out. Moreover, the CV curve of the MnO₂ in Figure 3b shows a pair current peaks at the potential range of 0.4-0.7 V, which is associated with the Faradaic redox reaction [34,35]. However, the CV curves of the 3DG/CB/MnO₂ composite show no significant redox peak at all the scan rate, indicating that the 3DG/CB/MnO₂ composite has a good charge-discharge cycling stability. Figure 4a exhibits the GCD curves of the 3DG/CB/MnO₂ composite at different current densities.

Figure 4a displays the GCD curves of the 3DG/CB/MnO₂ composite at different current densities. According to the method reported in literature [36], the calculated specific capacitance of the

3DG/CB/MnO₂ composite at the current densities of 0.3, 1 and 3 A/g is 590, 433 and 247 F/g, respectively. The GCD curves of the 3DG, MnO₂ and 3DG/CB/MnO₂ composite at 0.3 A/g are indicated in Figure 4b, which presents that the specific capacitance of the 3DG/CB/MnO₂ composite is far higher than that of the MnO₂ (433 F/g). This result obtains agree well with the CV test. Moreover, the GCD curve of the 3DG/CB/MnO₂ composite remains a symmetry at high current density very well, showing that the 3DG/CB/MnO₂ composite has excellent coulombic efficiency.

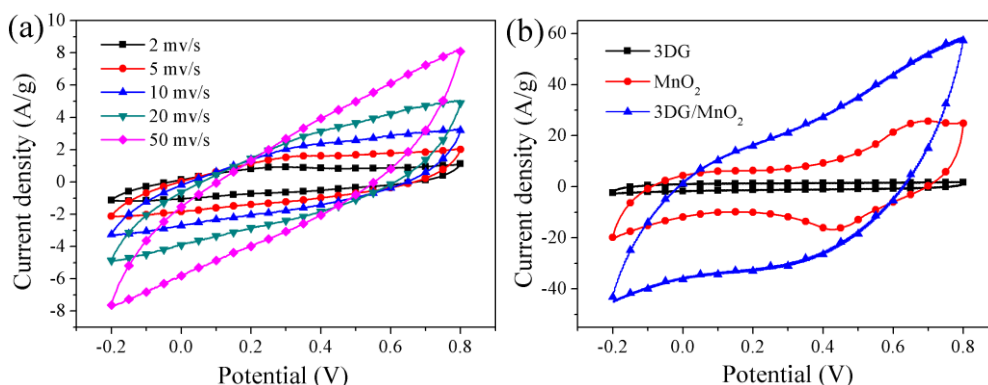


Figure 3. (a) CVs of the 3DG/CB/MnO₂ composite at different scanning rate. (b) CVs of the 3DG, MnO₂ and 3DG/CB/MnO₂ composite at 200 mV/s.

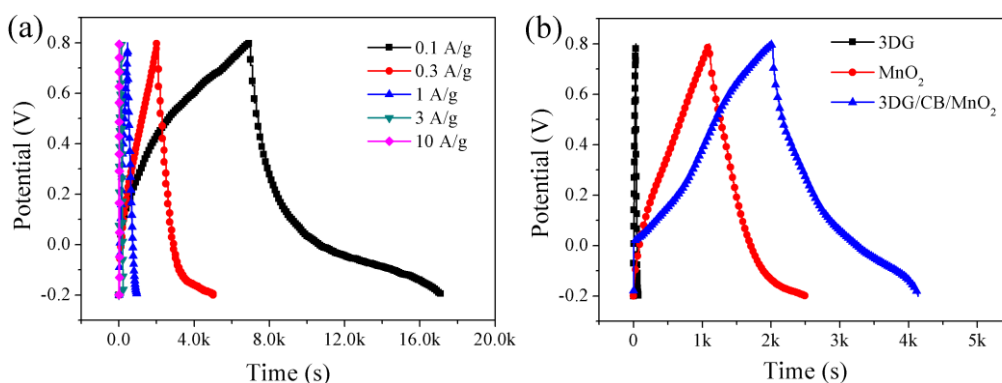


Figure 4. (a) GCD curves of the 3DG/CB/MnO₂ composite at different current densities. (b) GCD curves of the 3DG, MnO₂ and 3DG/CB/MnO₂ composite at 0.3 A/g.

Figure 5 presents the cycle curves of the MnO₂ and 3DG/CB/MnO₂ composite at the current density of 30 A/g for 5000 circles, which indicates the cycling stability of these electrode materials. After 3DG/CB/MnO₂ composite is charge-discharged at the high current density of 30 A/g for 5000 cycles, as can be seen from Figure 5, its specific capacitance decreases from 55 to 38 F/g, namely, its capacity retention rate is close to 70%. Under the same conditions, however, the capacitance retention rate of the MnO₂ is only 32%. These results show that the cycling stability of the 3DG/CB/MnO₂ composite is great better than that of the MnO₂. These results imply that, after charge-discharged at 30 A/g for 5000 cycles, the microstructure of the 3DG/CB/MnO₂ composite remains intact, and there is

not a large number of structural damage and collapse, due to the strong supporting role of the stable carbon network structure constructed by 3DG and carbon black in the microstructure of the 3DG/CB/MnO₂ composite [37].

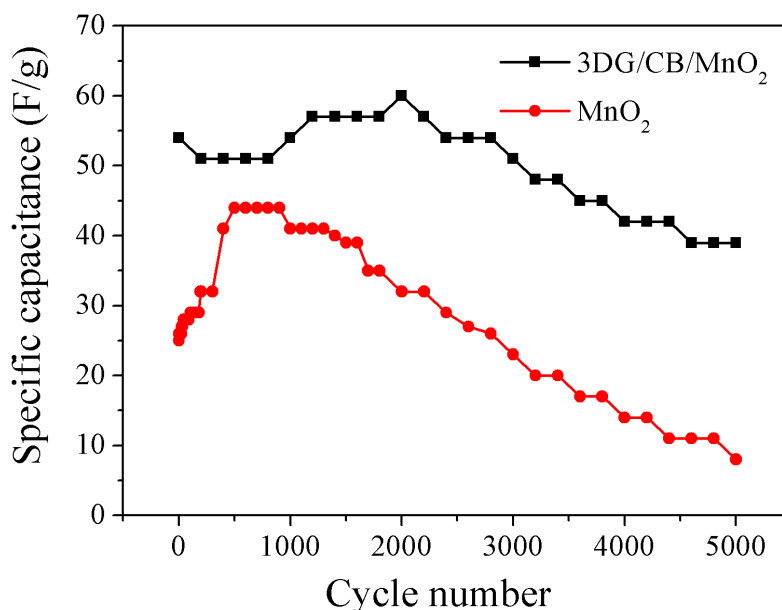


Figure 5. Cycle curves of the MnO₂ and 3DG/CB/MnO₂ composite at the current density of 30 A/g for 5000 circles.

4. CONCLUSION

Using the 3DG and commercial carbon black as a supporting structure material, the 3DG/CB/MnO₂ composite is synthesized by a hydrothermal method and successfully employed as an electrode material for supercapacity. In the composite material, MnO₂ nanoparticles are grown with success on the surface of the 3DG. The specific capacitance and charge-discharge cycling stability of the 3DG/CB/MnO₂ composite are far better than those of the MnO₂, due to the synergistic effect between the carbon materials with large surface area and pseudocapacitive MnO₂. The specific capacitance of the 3DG/CB/MnO₂ composite at the current densities of 0.3, 1 and 3 A/g is 590, 433 and 247 F/g, respectively. Moreover, after charge-discharged at 30 A/g for 5000 cycles, its capacity retention rate is close to 70%. The high specific capacitance and excellent cycling stability of the 3DG/CB/MnO₂ composite relate to its unique microstructures. On the one hand, the 3DG with porous structure can effectively support the pseudocapacitive MnO₂, ensuring the stability of the microstructure, and avoiding the contact between the electrode material and the electrolyte is not sufficient due to the stacking of the material; on the other hand, the carbon network structure constructed by 3DG and carbon black accelerates the transfer of Faraday charge.

ACKNOWLEDGEMENTS

This work is supported by the Scientific and Technological Innovation Programs of Higher Education Institutions in Shanxi (STIP, 2014113) and Natural Science Foundation of Shanxi (2014011017-2).

References

1. X. J. Wan, Y. Huang and Y. S. Chen, *Accounts Chem. Res.*, 45 (2012) 598.
2. W. K. Li and Y. J. Yang, *J. Solid State Electr.*, 18 (2014) 1621.
3. S. Yang, W. B. Yue, J. Zhu, Y. Ren and X. J. Yang, *Adv. Funct. Mater.*, 23, (2013) 3570.
4. Yin, H. S. Zhao, J. Wan, H. Tang, L. Chang, L. He, H. Zhao, Y. Gao and Z. Tang, *Adv. Mater.*, 25 (2013) 6270.
5. J. Jeong, J. Kim, H. Y. Noh, S. M. Jeong, J. H. Kim and S. Myung, *Aip Adv.*, 4 (2014) 097111.
6. D. X. Ye, L. Q. Luo, Y. P. Ding, B. D. Liu and X. Liu, *Analyst*, 137 (2012) 2840.
7. A. Torres, M. P. Lima, A. Fazzio and A. J. R. da Silva, Spin caloritronics in graphene with Mn. *Appl. Phys. Lett.* 104 (2014) 072412.
8. H. Liu, J. Huang, X. Li, J. Liu, Y. Zhang and K. Du, *Appl. Surf. Sci.*, 258 (2012) 4917.
9. H. Lee, J. K. Yoo, J. H. Park, J. H. Kim, K. Kang and Y. S. Jung, *Adv. Energy Mater.*, 2 (2012) 976.
10. L. Wu, R. Li, J. Guo, C. Zhou, W. Zhang, C. Wang, Y. Huang, Y. Li and J. Liu, *Aip Adv.*, 3 (2013) 082129.
11. Y. Gao, Y. S. Zhou, W. Xiong, L. J. Jiang, M. Mahjouri-samani, P. Thirugnanam, X. Huang, M. M. Wang, L. Jiang and Y. F. Lu, *Apl Mater.*, 1 (2013) 012101.
12. M. David-Pur, L. Bareket-Keren, G. Beit-Yaakov, , D. Raz-Prag and Y. Hanein, *Biomed. Microdevices*, 16 (2014) 43-53.
13. Q. Wang, J. Xu, X. Wang, B. Liu, X. Hou and G. Yu, *Chemelectrochem*, 1 (2014) 559.
14. M. Mao, J. Y. Hu and H. T. Liu, *Int. J. Energ. Res.*, 39 (2015) 727.
15. T. Cetinkaya, A. Akbulut, M. O. Guler and H. Akbulut, *J. Appl. Electrochem.*, 44 (2014) 209.
16. H. C. Gao and H. W. Duan, *Biosens. Bioelectron.*, 65 (2015) 404.
17. L. Zhang, F. Zhang, X. Yang, G. Long, Y. Wu, T. Zhang, K. Leng, Y. Huang, Y. Ma, A. Yu and Y. Chen, *Sci. Rep-Uk.*, 3 (2013) 1408.
18. X. Cao, Y. Shi, W. Shi, G. Lu, X. Huang, Q. Yan, Q. Zhang, H. Zhang, *Small*, 7 (2011) 3163.
19. K. G. Lee, J. M. Jeong, S. J. Lee, B. Yeom, M. K. Lee, B. G. Choi, *Ultrason. Sonochem.*, 22 (2015) 422.
20. X. Xie, C. Zhang, M. B. Wu and C. Yuan, *Chem. Commun.*, 49 (2013) 11092.
21. H. Sun, Y. Liu, Y. Yu, M. Ahmad, D. Nan and J. Zhu, *Electrochim. Acta*, 118 (2014) 1.
22. P. Si, X. C. Dong, P. Chen and D. Kim, *J. Mater. Chem. B*, 1 (2013) 110.
23. Z. X. Huang, Y. Wang, Y. G. Zhu, Y. Shi, J. I. Wong and H. Y. Yang, *Nanoscale*, 6 (2014) 9839.
24. B. Zhan, C. Liu, H. Chen, H. Shi, L. Wang, P. Chen, W. Huang and X. Dong, *Nanoscale*, 6 (2014) 7424.
25. Y. Ma, W. Chen, P. Zhang and E. Xie, *Rsc Adv.*, 4 (2014) 47609.
26. S. Devaraj and N. Munichandraiah, *J. Phys. Chem. C*, 112 (2008) 4406.
27. W. S. Hummers and R. E. Offeman, *J. Am. Chem. Soc.*, 80 (1958) 1339.
28. S. Yan, L. Gao, S. Zhang, W. Zhang, Y. Li and L. Gao, *Electrochim. Acta*, 94 (2013) 159.
29. S. Yan, L. Gao, S. Zhang, L. Gao, W. Zhang and Y. Li, *Int. J. Hydrogen Energy*, 38 (2013) 12838.
30. S. Yan, S. Zhang, W. Zhang, J. Li, L. Gao, Y. Yang and Y. Gao, *J. Phys. Chem. C*, 118 (2014) 29845.
31. X. Du, C. Zhou, H. Y. Liu and Y. W. Mai, *J. Power Sources*, 241 (2013) 460.
32. X. L. Li, G. Y. Zhang, X. D. Bai, X. M. Sun, X. R. Wang, E. Wang, and H. J. Dai, *Nat. Nanotechnol.*, 3 (2008) 538.

33. J. H. Liu, J. W. An, Y. X. Ma, M. L. Li, and R. B. Ma, *J. Electrochem. Soc.*, 159 (2012) A828-A833.
34. M. S. Wu, Z. S. Guo, J. J. Jow, *J. Phys. Chem. C*, 114 (2010) 21861.
35. Y. Y. Gao, S. L. Chen, D. X. Cao, G. L. Wang and J. L. Yin, *J. Power Sources*, 195 (2010) 1757.
36. L. T. Drzal, and S. Biswas, *Chem. Mater.*, 22 (2010) 5667.
37. X. Wang, Y. Zhang, C. Zhi, X. Wang, D. Tang, Y. Xu, Q. Weng, X. Jiang, M. Mitome, D. Golberg and Y. Bando, *Nat. Commun.*, 4 (2013) 1294.

© 2016 The Authors. Published by ESG (www.electrochemsci.org). This article is an open access article distributed under the terms and conditions of the Creative Commons Attribution license (<http://creativecommons.org/licenses/by/4.0/>).